Precision Measurements of Electroproduction of π^0 near Threshold: A Test of Chiral QCD Dynamics

An Update to Proposal E01-014

D. Crabb, D. Day, R. Lindgren (spokesperson) [1], N. Liyanage
B.E. Norum (spokesperson), O. Rondon-Aramayo, B. Sawatzky,
C. Smith, K. Wang

University of Virginia, Charlottesville, VA 22903, USA

W. Bertozzi, 0. Gayou, S. Gilad, P. Monaghan, R. Suleiman

Massachusetts Institute of Technology, Cambridge, MA 02139, USA

J. Watson, R. Subedi

Kent State University, Kent, Ohio, USA

S. Širca

Department of Physics, University of Ljubljana, Slovenia

J.R.M. Annand (spokesperson), D. Ireland, J. Kellie, K. Livingston,
G. Rosner

University of Glasgow, Glasgow, Scotland, UK

D. Watts

University of Edinburgh, Edinburgh, Scotland, UK

V. Nelyubin (spokesperson) [2]

St. Petersburg Nuclear Physics Institute, Gatchina, Russia

I.I. Strakovsky, R.A. Arndt, W.J. Briscoe, R.L. Workman

The George Washington University, Washington, DC 20052, USA

Ulf-G. Meißner

Universität Bonn, Helmholtz-Institut für Strahlen- und Kernphysik, Bonn, Germany
Forschungszentrum Jülich Institut für Kernphysik, D-52425 Jülich, Germany

Jefferson Lab PAC25 Proposal *2 December 2003*

J.P. Chen, R. Feuerbach, J. Gomez, J.-O. Hansen,
D.W. Higinbotham (spokesperson), C.W. de Jager, J. LeRose
R. Michaels, S. Nanda, B. Reitz, A. Saha, B. Wojtsekhowski

Jefferson Lab, Newport News, VA 22606, USA

J. Goity

Hampton University, Hampton, VA 23668, USA

L. Bimbot

Institut de Physique Nucleaire, F-91406 Orsay Cedex, France

K.G. Fissum

University of Lund, Box 118, SE-221 00 Lund, Sweden

I.A. Rachek [3]

Budker Institute, Novosibirsk, Russia

X. Jiang, R. Ransome

Rutgers University, New Brunswick, NJ 08903, USA

E. Piasetzky

Tel Aviv, Israel

N. Kolb, R. Igarashi, R. Pywell

University of Saskatchewan, Saskatoon, Canada

K. Egiyan, V. Mamyan, S. Mailyan, A. Shahinyan, H. Voskanyan

Yerevan Physcis Institute

and

The Hall-A Collaboration

Abstract

This proposal is an update of experiment E01-014. We propose to make a high precision measurement of the reaction p(e,e'p)π^0 near threshold in a fine grid of Q^2 and ΔW in the range of $0.04\ [GeV/c]^2 \leq Q^2 \leq 0.14\ [GeV/c]^2$ and $0\ MeV \leq \Delta W \leq 20\ MeV$. The experiment will be performed in Hall-A using an HRS spectrometer in coincidence with the BigBite spectrometer. A new set of wire chambers, funded by an NSF MRI grant, is currently being constructed to enable us to take full advantage of the large acceptance of the BigBite. This will enable us to make all measurements with the spectrometers in a single configuration thereby minimizing systematic uncertainties. The structure functions $\sigma_T+\epsilon_L\sigma_L$, σ_{TL}, and σ_{TT} will be extracted using the ϕ dependence of the differential cross sections. The results will provide a stringent test of chiral QCD dynamics, a test made all the more critical by recent measurements showing disagreement with the predictions of Chiral Perturbation Theory. This fine grid of results in Q^2 and ΔW will also provide valuable input to the MAID and SAID partial wave analysis codes.

Contents

[1] contact person: R.A. Lindgren, phone: 804-982-2691, e-mail: lindgren@jlab.org
[2] supported by Jefferson Lab and the University of Virginia
[3] supported by Jefferson Lab

1 Introduction

During the last several years significant progress has been made in the application of QCD in the non-perturbative regime via the use of effective Chiral Perturbation Theory (ChPT). Many examples of theoretical progress and the comparison to experiment were recently presented at the Chiral Dynamics 2003 Workshop [1]. Applied to the π-N system, ChPT starts with a Lagrangian embodying the underlying symmetries of QCD expressed in terms of the relevant degrees of freedom: the pion and the nucleon. Scattering or production processes can be described in terms of small quantities like Q/M, where Q is the four-momentum transferred to the π-N system, and m_π/M, the latter reflecting the explicit symmetry breaking through the current quark masses in L_{QCD}. Since it involves the well understood electromagnetic interaction and small kinematic quantities, near-threshold electromagnetic production of pions (in particular, neutral pions due to the absence of the overshadowing Kroll-Ruderman term) from nucleons provides an ideal testing ground for ChPT. As ChPT is an "effective" field theory, the description of pion electroproduction contains parameters, the so-called Low Energy Constants or LEC's, which must be fixed by measurement. However, once these are fixed it should be possible to predict consistently the evolution with Q^2 and W (center-of-mass energy of the π-N system) of all observables.

The goal of the proposed measurements is to measure precisely the reaction $p(e,e'p)\pi^0$ from threshold to ΔW = 20 MeV above threshold for a range of momentum transfers encompassing those of the Mainz data ($Q^2 = 0.05[GeV/c]^2$ and $Q^2 = 0.10[GeV/c]^2$), and extending to both lower and higher values: $0.04\ [GeV/c]^2 \leq Q^2 \leq 0.14[GeV/c]^2$. These data will enable us to either confirm or refute the existence of a significant discrepancy with the predictions of ChPT and, depending upon the result, either investigate the source of the discrepancy or test the ability of ChPT to predict higher P–wave contributions.

The extraction of cross sections from near threshold requires precise determination of the reaction product momenta. In addition, since the near threshold cross sections are relatively small, high luminosity, high beam energy, and as large acceptance as possible are desirable. Hall A, with the HRS and BigBite spectrometer, singularly satisfies these requirements. Hall A of Jefferson Lab provides the foremost facility capable of providing the necessary resolution as well as systematic and statistical precision.

2 Overview

Considerable effort has gone into measurements of both the photoproduction $p\,(\gamma,\pi^0)$ and electroproduction $p(e,e'p)\pi^0$ of neutral pions near threshold. Measurements at Mainz [2] and Saskatoon [3] of the lowest contributing multipole (E_{0^+}) to photoproduction are well reproduced by ChPT. On the other hand, high precision measurements at Mainz of electroproduction with four-momentum transfers of 0.10 $[GeV/c]^2$ [4] and 0.05 $[GeV/c]^2$ [5,6]

tell a different story. ChPT calculations were fit to the $Q^2 = 0.10[GeV/c]^2$ data [4] and the LEC's were determined. It was thus surprising to discover that ChPT predictions of the $Q^2 = 0.05[GeV/c]^2$ measurements [5,6] disagreed significantly. Discrepancies were observed both at threshold (the value of the L_{0^+} multipole was observed to be twice the predicted value) and at higher values of W where the P–wave contributions are significant. It was also reported in the previous work [6] that measurements were repeated at a different virtual photon polarization. The conclusion was that similar results were obtained and the data are still in disagreement with Heavy Baryon Chiral perturbation theory (HBChPT). These data are also inconsistent with the predictions of the SAID analysis [7,8] and MAID model [9]. If these discrepancies remain unresolved, they will constitute a serious threat to the viability of ChPT as a useful theory of dynamical processes. Such a result would be problematical as ChPT is firmly grounded in the basic properties of QCD.

To preform a new, high precision threshold pion production experiment in Hall A will require the large acceptance BigBite spectrometer [10,11], the High Resolution Spectrometers (left HRS and right HRS) with septum magnets (constructed for experiments [12–14]), and the highly segmented lead glass calorimeter (constructed for experiment [15]). Due to the BigBite spectrometer's 96 msr solid angle acceptance and 80% momentum acceptance, the entire proton angular distribution can be measured within a single kinematic setting, thus minimizing systemic errors associated with spectrometer movements. This differs greatly from previous Mainz measurements, where several spectrometer positions were required to cover the necessary angular range. Two six-plane multi-wire drift chambers with spatial position resolution of the order of 0.2 mm and proton emission angular resolution of a few milliradians are under construction for BigBite. The septum magnet will enable the Hall-A spectrometers to reach small scattering angles (6 degrees) so relatively high beam energies can be used, thus maximizing the cross section for a given value of Q^2. The lead glass calorimeter will be used to calibrate the acceptance of BigBite. A modified Hall A liquid cryogenic hydrogen target with thinner cell windows made of Havar to minimize multiple scattering of low energy protons along with a new scattering chamber will be used.

This combination of equipment will allow neutral pion electro-production cross sections to be measured near threshold on a fine grid of four momentum transfer, pion momentum and angle in the pion-nucleon center of mass system. The measurements proposed herein will cover the four momentum transfer range $Q^2 = 0.04$ - 0.14 $[GeV/c]^2$ and the invariant mass range $\Delta W = 0 - 20$ MeV above threshold. The ϕ dependence of the cross section will be used to extract the structure functions $\sigma_T + \epsilon_L \sigma_L$, σ_{TL}, and σ_{TT}.

3 Motivation

3.1 Theory

Quantum Chromodynamics (QCD) is the fundamental and, in principal, complete theory which describes hadron-hadron interactions in terms of the underlying dynamics of the quark-gluon degrees of freedom. However, the essentially nonperturbative nature of QCD presents a formidable challenge. One approach to describing strong interaction phenomena is through phenomenological models. Another is through the use of an Effective Field Theory (EFT) constrained by the fundamental symmetries of QCD. In the low energy regime, QCD exhibits approximate chiral symmetry which is spontaneously broken by the existence of massive Goldstone bosons: pion, kaons, eta. Nevertheless, the interactions between hadrons and pions are constrained by chiral symmetry. This enables one to expand about the chiral limit relevant amplitudes in power series in m_π/M, the ratio of the pion mass (m_π) to nucleon mass (M), and q/M, where q represents any (presumably small) momentum or mass appearing in the problem. This approach is called Chiral Perturbation Theory (ChPT); strictly speaking, it is Heavy Baryon CHPT (HBChPT). Because ChPT is an effective theory certain details of the interaction are masked when one calculates beyond the leading or tree level. The effects are absorbed into empirically determined constants, the so-called Low Energy Constants (LEC's), the magnitudes of which determine the importance of the higher level terms. Once these constants have been determined from measurements of a process for one set of kinematics, one should in principle be able to predict the amplitudes involved for other kinematical conditions.

Calculations within ChPT are necessarily expansions, so the questions of how many powers must be retained and of how many loops beyond the tree level must be kept remain. The only practical way to address this problem is to perform measurements under conditions where the factors governing the expansion are small. In the case of pion electro-production from the proton, this occurs when Q^2, the 4-momentum transfer, and $\Delta W = W - M - m_\pi$, the energy above threshold of the final state, are both small. By using a measurement made under such conditions to fix the LEC's, and then comparing the predictions made using them to measurements made under different kinematics one can establish the range of validity of the underlying approach. Significantly, it will determine the range over which ChPT can be used as a guide to lattice gauge calculations.

Examination of existing threshold electro- and photo-production data shows that progress is being made, but that serious inconsistencies remain [16]. For example, in the recent studies performed at Mainz, data taken at $Q^2 = 0.10[GeV/c]^2$ [4] were used to determine the LEC's. Using these values, predictions were made for the S–wave and P–wave amplitudes at $Q^2 = 0.05[GeV/c]^2$. The results of these comparisons are presented below.

3.1.1 S–Wave Amplitudes

Near threshold, neutral pion production cross section is dominated by the S–wave amplitudes E_{0+} and L_{0+}; at threshold these are all that survive. Fig. 1 shows the existing high precision measurements of the total neutral pion production cross section as a function of ΔW and Q^2. The solid curve labeled ChPT was computed [17,18] using LEC's determined from measurements at $Q^2 = 0.10\ [GeV/c]^2$ reported in reference [4]. The marked disagreement between the calculation and the precise data from Mainz [6] at $Q^2 = 0.05[GeV/c]^2$ is striking. Figure 2 shows the individual E_{0+} and L_{0+} amplitudes extracted from the data of reference [4]. Neither the ChPT calculation nor the MAID parameterization provides good representations of the data.

The disagreement gives rise to several questions. First, is it necessary at $Q^2 = 0.10\ [GeV/c]^2$ to include a significantly larger number of terms in the Chiral expansion, thereby increasing the number of LEC's to be determined empirically? If new, precise data spanning the range around $Q^2 = 0.05[GeV/c]^2$ were to be used to determine the LEC's and the resulting calculation were to reproduce the Q^2 evolution of the data in this region but to fail increasingly as Q^2 approaches $0.10\ [GeV/c]^2$ then this explanation would be favored. Second, is something basically wrong with the ChPT formulation? Again, if new, precise data in the range $0.04\ [GeV/c]^2 \leq Q^2 \leq 0.14\ [GeV/c]^2$ cannot be reproduced then this explanation would be favored. Third, is it possible that one or more data points are in error? This question can only be answered by obtaining new, high statistics data taken under conditions which minimize systematic uncertainties.

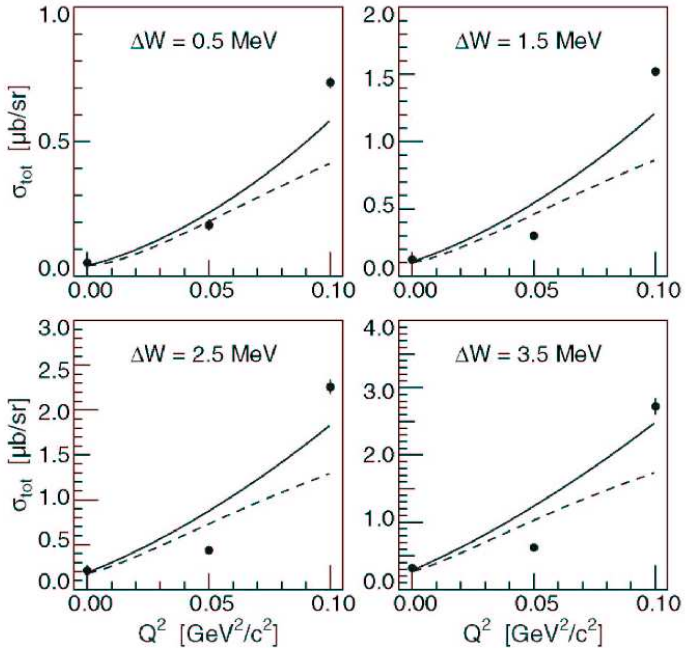

Fig. 1. The W and Q^2 dependence of the total cross section at $\epsilon = 0.8$. The solid(dashed) line is the prediction of ChPT (MAID). This figure is taken from Ref. [6] The proposed experiment will measure these total cross sections in bins of $0.01\ [GeV/c]^2$ from 0.04 to $0.14\ [GeV/c]^2$ in order to answer the aforemented questions.

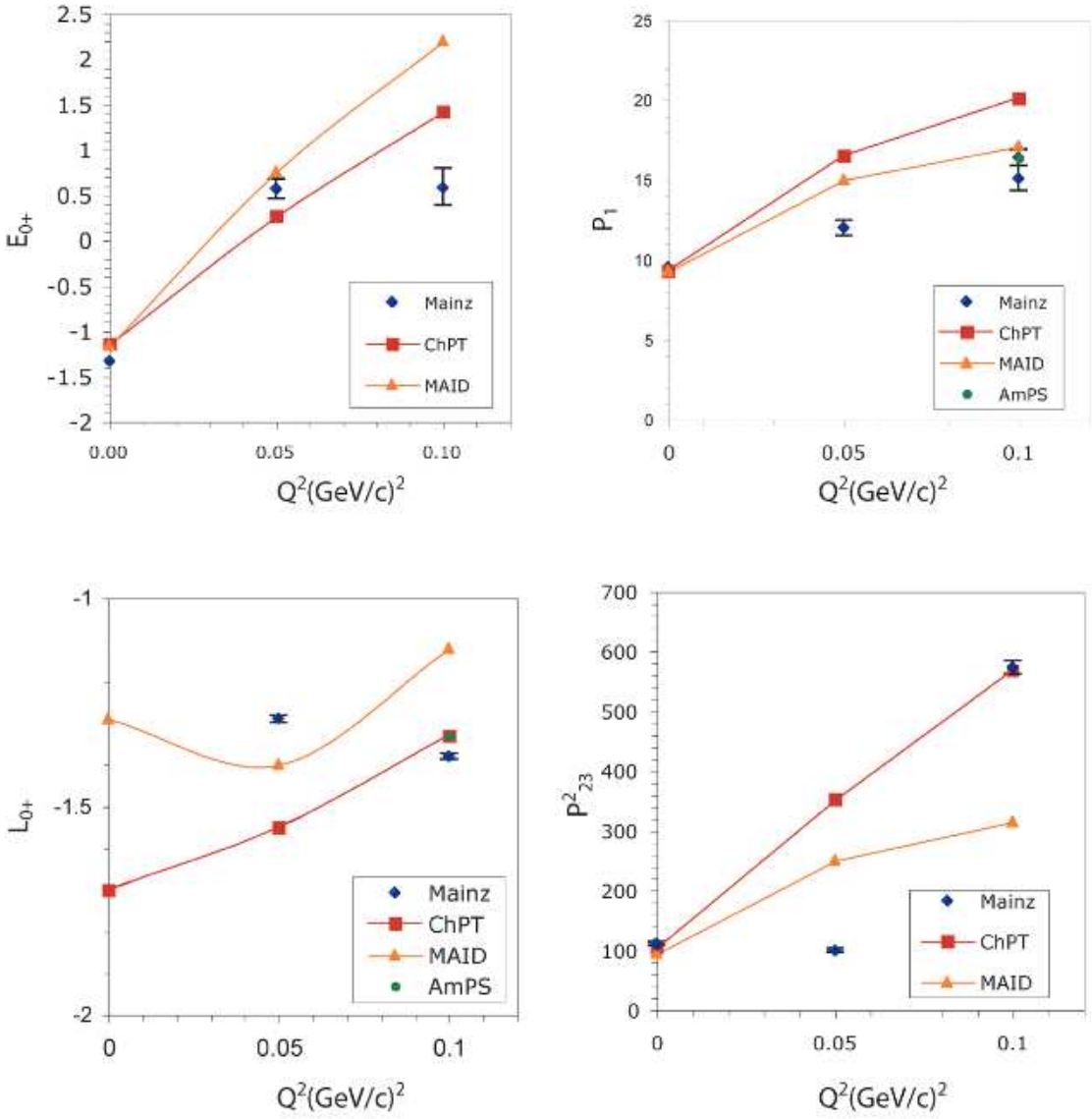

Fig. 2. On the left the S-wave amplitudes E_{0+} and L_{0+} are plotted versus Q^2. On the right the P-wave amplitude P_1 and the combination $P_{23}^2 = 1/2(P_2^2 + P_3^2)$ are plotted versus Q^2. The Mainz data for $Q^2 = 0.10$ and 0.05 $[GeV/c]^2$ are from references [4] and [6]. The AmPS NIKHEF data are from reference [19].

3.1.2 P–Wave Amplitudes

In 1996 Bernard [20] pointed out that because the calculated S–wave E_{0+} is a slowly converging function of m_π/M, it currently is not necessarily the best observable with which to test ChPT. Until one is confident that the computation of an amplitude has converged, it is not clear what one learns by a comparison with data. In contrast, the calculations of the P–wave multipoles converge much more rapidly. In the low energy expansion, these multipoles have been calculated through next-to-leading order. This makes them much more attractive for tests of ChPT. There are five P-wave multipoles: E_{1+}, $M_{1\pm}$, and $L_{1\pm}$. In both the Mainz and NIKHEF extractions of E_{0+} and L_{0+} for $Q^2 = 0.10\ [GeV/c]^2$, the calculated P-wave contributions of ref. [21] were assumed.

Evidence that the P-waves are not well understood derives from comparing specifically the values of P_1 and the combination $P_{23}^2 = 1/2(P_2^2 + P_3^2)$ extracted from the data to the corresponding ChPT and MAID predictions. These comparisons are shown in Fig. 2. Once again, there exist very large discrepancies between experiment and theory.

It is also instructive to look at the evolution of the discrepancy between experiment and ChPT predictions as the energy in the final proton-pion state increases from threshold. Fig. 3 shows the measured [6] differential longitudinal-transverse cross section at $Q^2 = 0.05\ [GeV/c]^2$ for four energy bins above threshold compared to the predictions of ChPT. Here again, the LEC's appearing in the ChPT calculation were extracted from the measurements at $Q^2 = 0.10\ [GeV/c]^2$. Here again, there are striking discrepancies. It is notable that the discrepancies get worse as the energy above threshold increases. Since the contributions of the P-waves increase with energy above threshold, the observed discrepancies suggest a serious problem with the P-waves.

To obtain a better understanding of the S– and P–wave contributions to the cross sections, it is necessary to gather more precise data in the threshold region, i.e., for final state energies $0 \leq \Delta W \leq 20$ MeV and on a much finer grid of Q^2 in the range $0 \leq Q^2 \leq 0.1\ [GeV/c]^2$. A better understanding of these amplitudes and the ability of ChPT to reproduce them will ultimately deepen our understanding of QCD in the non–perturbative regime [16].

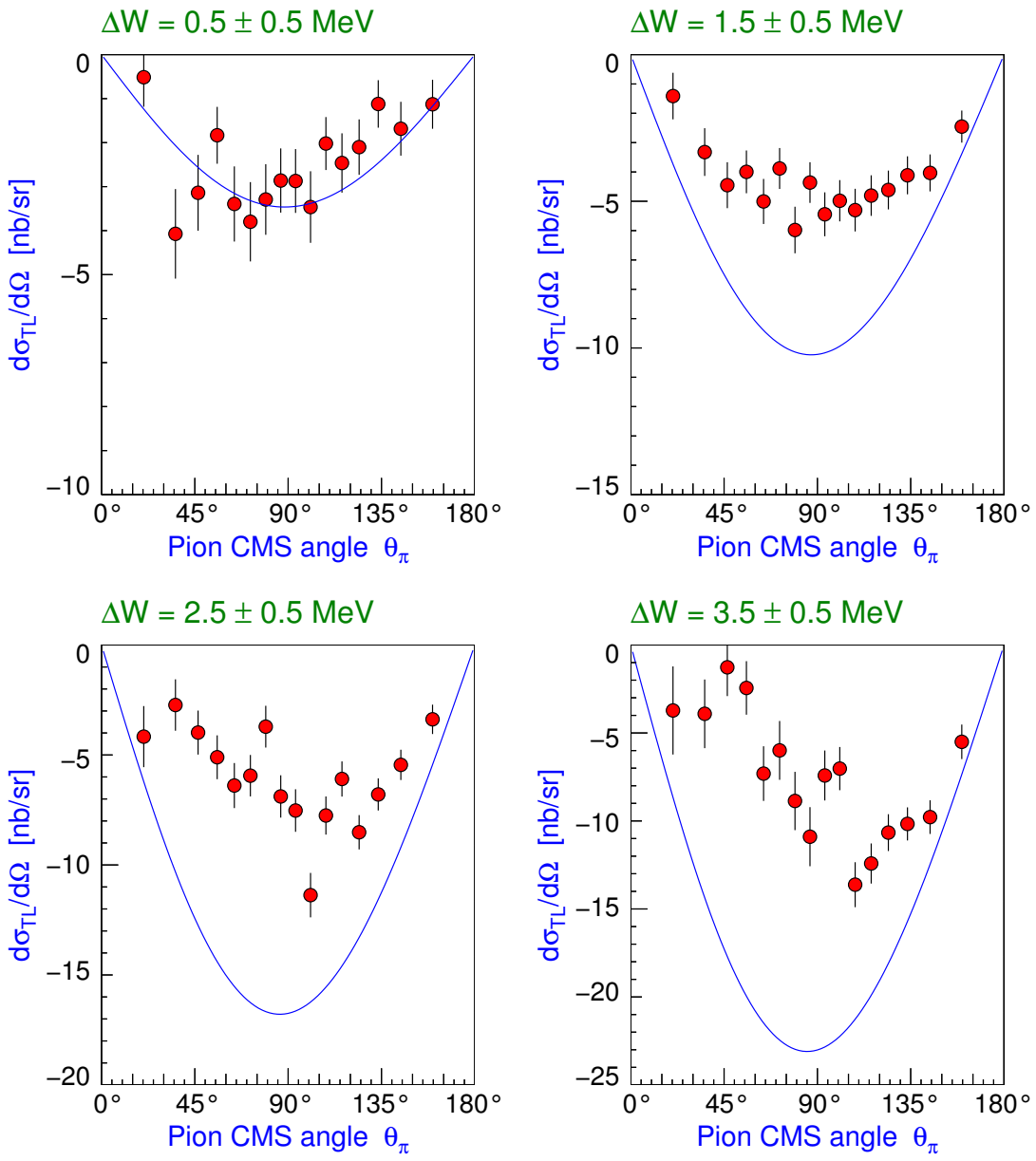

Fig. 3. Differential longitudinal-transverse cross section for $Q^2 = 0.05\ [GeV/c]^2$ and different final state energy bins measured at Mainz [6]. The solid lines are the results of ChPT [17] calculations for which the required LEC's were derived from measurements at $Q^2 = 0.10\ [GeV/c]^2$. Large discrepancies which increase with the final state energy are observed.

3.1.3 Partial Wave Analysis

In a partial wave analysis, as performed in the SAID [22] and MAID [9] calculations, the cross section is written as an expansion in terms of six helicity amplitudes [23,9]. Each amplitude is given in a partial wave expansion of products of the electric ($E_{l\pm}$), magnetic ($M_{l\pm}$), and longitudinal ($L_{l\pm}$) multipole amplitudes as well as the derivatives of Legendre polynomials. Here, l is the relative pion-nucleon angular momentum and $j = l \pm \frac{1}{2}$ is the total angular momentum. The production amplitudes are determined by fits to the data. The two main sources of experimental data near threshold are NIKHEF [24] and Mainz [4].

In Fig. 4, the Mainz 1998 differential cross-section data are shown [4] as a function of the pion center of mass polar angle and are compared to the SAID [22] and MAID [9] predictions. Clearly, the data are not fit well by either calculation. Moreover, there appears to be a decrease in the data at forward angles that is qualitatively inconsistent with both calculations. Adjustments to the pion multipole amplitudes as shown in Fig. 5 are not sufficient to bring the calculations into agreement with the data. Neither SAID nor MAID includes chiral loops consistently although some are included via unitarity. Thus, it would not be shocking if these calculations failed to work even at $Q^2 = 0.1$ $[GeV/c]^2$. Should these analyses prove unable to accommodate low-Q^2 data, the residual discrepancies could provide information about the chiral loop contributions. However, the current uncertainties are too large to draw any such conclusions. Data of much higher precision will be required to extract meaningful information from this apparent discrepancy.

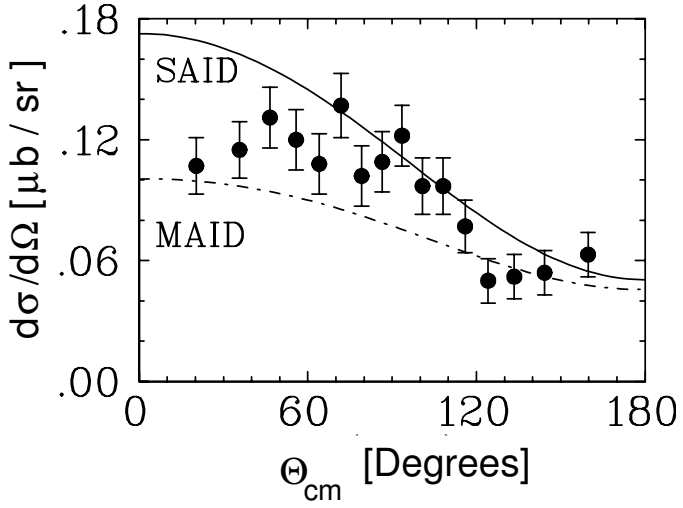

Fig. 4. Differential cross section data from Mainz [4] taken at Q^2=0.1 [GeV/c]^2 with Δ W = 1 MeV - 2 MeV. The solid and dot-dash curve are the predictions from the SAID [22] and MAID [9] parametrizations.

By performing a full partial wave analysis of the data to be obtained in the proposed experiment, the various multipole contributions can be determined precisely. As a point of reference, Fig. 5 shows the sensitivity of the cross section, as a function of the center of mass angle of the pion, to the contribution of the P_{33} multipole.

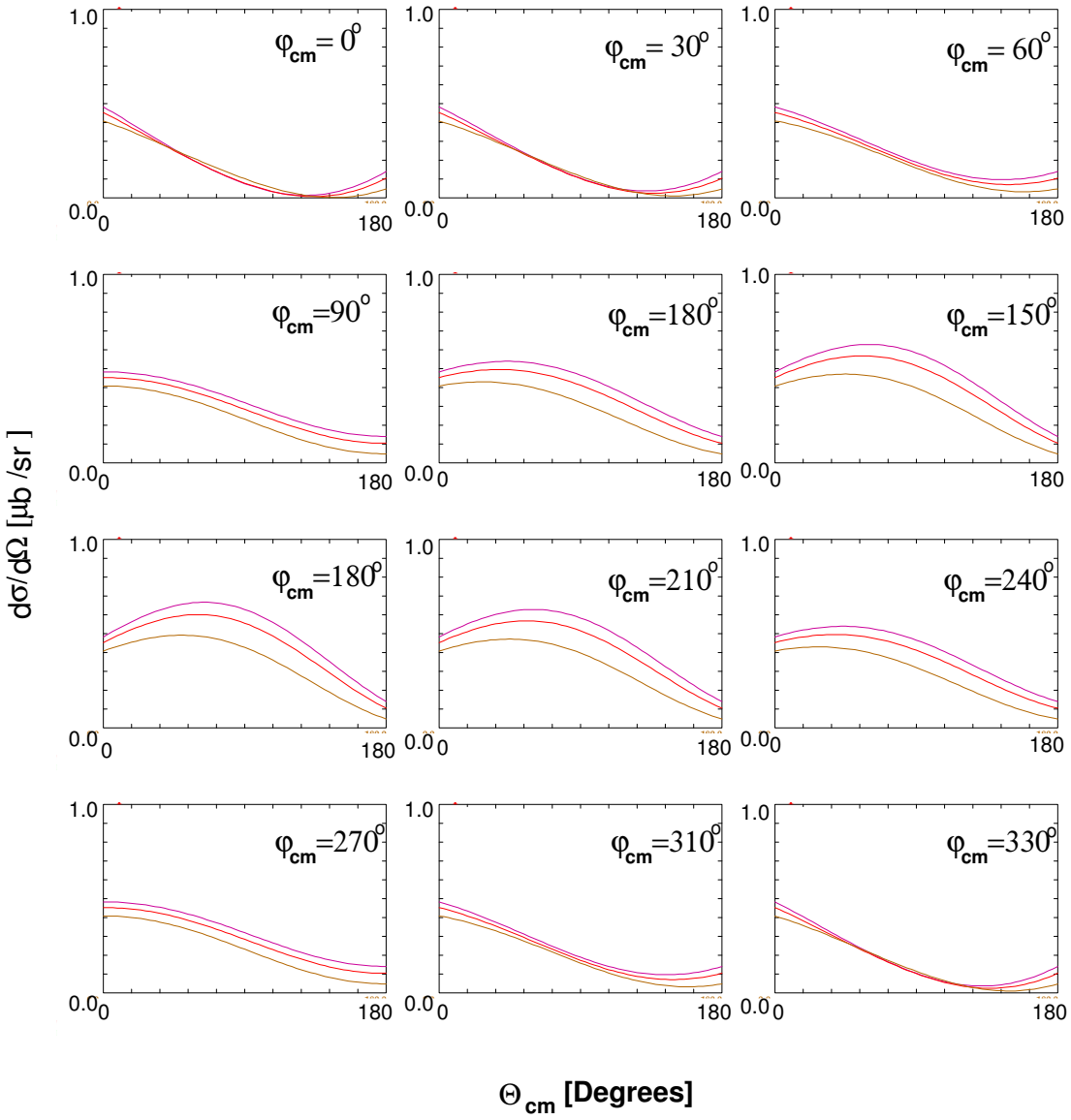

Fig. 5. The dependence of the differential cross section for a variation in the P_{33} contribution at $\Delta W = 5$ MeV, Q^2=0.10 [GeV/c]^2 as a function of θ_{cm} and ϕ_{cm}. These calculations were produced using SAID [22]. The upper, middle, and lower curves correspond to calculations done by reducing the modulus of the amplitude by 0%, 10% and 30%, respectively.

With the availability of high-duty-cycle, medium energy electron accelerators, some progress has been made in determining near-threshold cross sections during the last decade. The characteristics of several threshold experiments are summarized in Table 1. Measurements of $\gamma + p \rightarrow p + \pi^0$ at Mainz [2] and Saskatoon [3] have yielded values of the E_{0+}multipole. Ref. [3] is in good agreement with ChPT and also the SAID database fit [22]. And, after a period of some confusion, near-threshold cross sections are converging to a consensus value.

Compared to photoproduction, electroproduction of π^0's can, in principle, yield a great deal more information, thus permitting a more detailed comparison with theory. Unpolarized $\gamma^* + p \rightarrow p + \pi^0$ differential cross section measurements give four (as opposed to one) structure functions, the E_{0+} and L_{0+} multipoles, and the dependence on Q^2. However, high-accuracy differential cross section measurements over a broad kinematic range are necessary to provide a meaningful comparison with theory.

Table 1
List of threshold $\gamma, \gamma^* + p \rightarrow p + \pi^0$ measurements. Here, Q is the four-momentum transfer, $\Delta\ W$ is the energy above threshold and ϕ is the azimuthal pion emission angle in degrees.

Facility	Q^2 [GeV/c]^2	ΔW [MeV]	ϕ	Ref.	Comment
Mainz	0.0	0–110	N.A.	[2]	E_{0+}, ChPT
Saskatoon	0.0	3–20	N.A.	[3]	E_{0+}, ChPT
NIKHEF	0.04, 0.1	0–2.5	0	[19]	1% duty cycle
NIKHEF	0.1	1–14	0, 180	[24]	E_{0+}, L_{0+}, ChPT
Mainz	0.1	≤ 4	0	[4]	L-T sep., E_{0+}, L_{0+}, ChPT
Mainz	0.05	≤ 4	0	[6]	Q^2 dependence ChPT

At NIKHEF, following an experiment using the low duty factor linac directly [19], $p(e,e'p)\pi^0$ differential cross sections $d\sigma/d\Omega_\pi(\theta_\pi, \phi_\pi, W)$ were measured [24] at $Q^2 = 0.1$ GeV^2 using a 30% duty cycle beam from the AmPS stretcher ring and two high-resolution magnetic spectrometers. Close to threshold, the final-state proton emerges in a narrow cone around $\vec{q}$ so a relatively large coverage of phase space can be achieved even with spectrometers having relatively small acceptances. The E_{0+} and L_{0+} multipoles were extracted from the θ and ϕ cross-section dependencies, assuming P–wave multipole values obtained from theoretical predictions. A maximum model dependence of 10% was estimated. Similar measurements, also at $Q^2 = 0.1$ GeV^2, were made at the Mainz MAMI-B microtron [4]. The proton spectrometer covered all of phase space up to $\Delta W = 4$ MeV. In this case, a Rosenbluth separation was made and $d\sigma/d\Omega_\pi(\theta_\pi)$ obtained for T, L, LT and TT components. The systematic uncertainties in this experiment, which arose mainly from uncertainties in the electron beam energy and in the calibration of the electron spectrometer, were estimated to be about 20% at ΔW$\leq$1 MeV and to decrease as ΔW increased. The extracted experimental results for the LT component are shown in Fig. 3. New measurements [5,6] were made at Mainz at $Q^2 = 0.05[GeV/c]^2$ over the range of ΔW from 0-4 MeV. A Rosenbluth separation was made and $d\sigma/d\Omega_\pi(\theta_\pi)$ obtained for T, L,

LT and TT components. Systematic uncertainties were determined to be at the level of $d\sigma/\sigma = 20\%$ (10%, 5%, 3%) for a final state energy bin 1 MeV wide and centered on $\Delta W = 0.5\ MeV$ (1.5 MeV, 2.5 MeV, 3.5 MeV). It was also reported in this work [6] that measurements were repeated at a different virtual photon polarization ($\epsilon = 0.92$) and similar results were obtained.

A variety of pion electro-production experiments on the proton have been approved by Jefferson Lab PAC. However, these experiments focus on the resonance region rather than the threshold region. The CLAS detector of Hall B is limited to $Q^2 > 0.4$ GeV^2, mainly by target thickness, and cannot go much above luminosities of $\sim 10^{34}$cm^{-2}s^{-1}. Experiments at MIT-Bates also focus on the resonance region. There is currently no approved Jefferson Lab experiment to probe this reaction in the low Q^2 threshold region.

To study the $p(e,e'p)\pi^0$ reaction at threshold, we propose to use the large acceptance BigBite spectrometer to detect the proton and the left HRS preceded by the septum magnet to detect the electron as shown in Fig. 6. The high momentum resolution of the electron spectrometer left HRS will allow a precise determination of the invariant mass W and three momentum transfer $\vec{q}$. The large acceptance (90 msr) and momentum range (200 - 900 MeV/c) of BigBite will permit a large fraction of the cone of forward-emitted protons along $\vec{q}$ to be detected simultaneously. The front and back multi-wire drift chambers together with the magnet will allow precise reconstruction of the proton emission angles from the target. The ΔE and E scintillator planes will give particle identification information as well as time-of-flight information. The Hall-A standard 15 cm long liquid hydrogen target will be replaced by a modified version that will be 10 cm long and 2 cm wide with thin Havar windows and walls. The right HRS will be used as a single arm electron detector to monitor the luminosity during the experiment. The lead-glass calorimeter, developed for the $p(\gamma,\gamma)$ experiment[15], will be used as an electron arm in coincidence with BigBite to calibrate the BigBite spectrometer's angular and momentum acceptances.

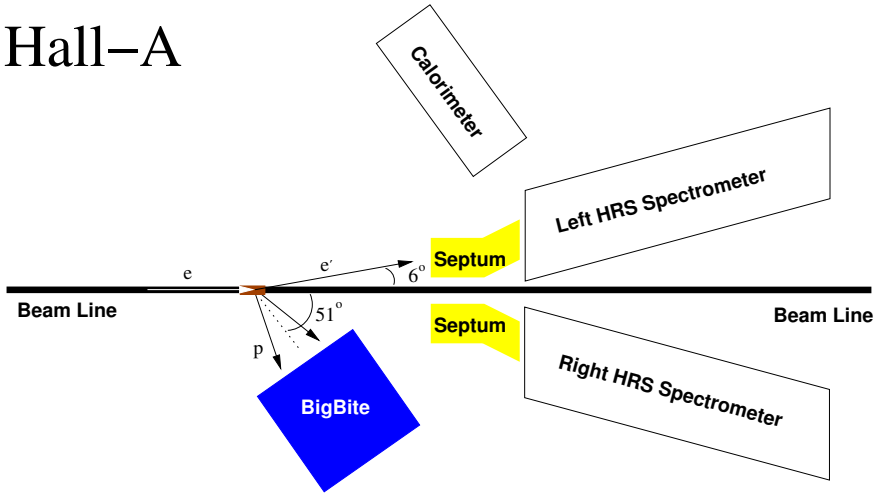

Fig. 6. For the $p(e,e'p)\pi^0$ experiment, the left HRS, the right HRS, and the calorimeter will be used as electron detectors and the BigBite spectrometer will be used as a proton detector. The left HRS will be used in coincidence with BigBite for measurement of the $p(e,ep')\pi^0$ reaction. The calorimeter will be used in coincidence with BigBite in order to calibrate the energy and acceptance of the new spectrometer. The right HRS will be used to monitor the luminosity of the experiment. A 10 cm long liquid Hydrogen target will be used.

The five-fold differential cross section for pion electro-production using an unpolarized electron beam can be written as [25],

$$\frac{d\sigma}{d\Omega_e d\Omega_\pi^* dE'} = \Gamma \frac{d\sigma_v}{d\Omega_\pi^*},$$

where,

$$\frac{d\sigma_v}{d\Omega_\pi^*} = \frac{d\sigma_T}{d\Omega_\pi^*} + \epsilon_L \frac{d\sigma_L}{d\Omega_\pi^*} + [2\epsilon_L(1+\epsilon)]^{1/2} \frac{d\sigma_{TL}}{d\Omega_\pi^*} \cos\phi + \epsilon \frac{d\sigma_{TT}}{d\Omega_\pi^*} \cos 2\phi.$$

A short hand notation for the T, L, TL, and TT two fold differential cross sections in the above formula are σ_T, σ_L, σ_{TL}, and σ_{TT}, respectively. The electron variables are defined in the laboratory system and the pion variables are defined in the pion-nucleon center of mass system designated by *, as shown schematically in Fig. 7. The two-fold differential cross sections (or structure functions) are defined in terms of the pion multipole amplitudes [25], which are functions of the two kinematic variables W, the invariant mass or cm energy of the pion-nucleon system, and the four momentum Q^2. These quantities are defined as,

$$W^2 = -Q^2 + 2m\nu + m^2,$$

$$Q^2 = 4EE' \sin^2 \frac{\theta_e}{2},$$

where m is the proton mass, $\nu = E - E'$, $Q^2 = -q^2$, $q^2 = \nu^2 - |\vec{q}|^2$, θ_e is the electron scattering angle, E is the electron beam energy, and E′ is the scattered electron energy, which is defined as,

$$E' = \frac{E - \frac{W^2 - m^2}{2m}}{1 + \frac{2E}{m} \sin^2 \frac{\theta_e}{2}}.$$

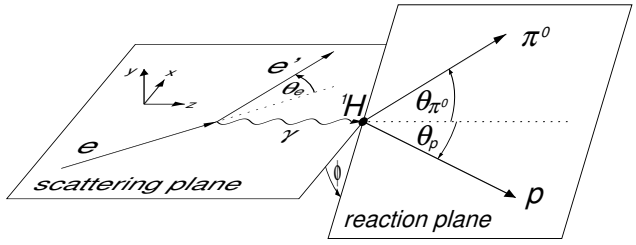

Fig. 7. A schematic of the electron scattering and pion-nucleon reaction plane

The transverse and longitudinal photon polarization parameters, ϵ and ϵ_L, and the virtual flux factor, Γ are defined as,

$$\epsilon = \frac{1}{1 + 2\vec{q}^2/Q^2 \tan^2 \frac{\theta_e}{2}},$$

$$\epsilon_L = \frac{Q^2}{\nu_{cm}^2}\epsilon,$$
$$\Gamma = \frac{\alpha E' k_\gamma}{2\pi^2 E Q^2 (1-\epsilon)},$$

with

$$k_\gamma = \frac{W^2 - m^2}{2m},$$
$$\nu_{cm} = \frac{W^2 - m^2 - Q^2}{2W}.$$

The out of plane ϕ dependence of the cross section will be used to separate and determine the structure functions $\sigma_T + \epsilon_L \sigma_L$, σ_{TT}, and σ_{TL}. Because epsilon is 0.99, the helicity dependent $\sigma_{TL'}$ structure function will not be determined and, therefore, only unpolarized beam will be considered. Threshold measurements will be made as a function of Q^2 and W. The minimum energy, W_{th}, to produce a pion in the CM is $W_{th} = m + m_{\pi^0} = 1073.26 MeV$. The CM energy above threshold is denoted by $\Delta W = W - W_{th}$.

4.2 Kinematics

In the Lab the kinematics of pion production near threshold have the feature that the recoil protons leave the interaction point in a narrow cone centered around the direction of the virtual photon momentum. The opening angle of this cone depends on W and $\vec{q}$ values. At 1 MeV above threshold, $\Delta W = 1$ MeV and $Q^2 = 0.04$, the angle of the cone relative to $\vec{q}$ is about 3.4° The magnitudes of $\vec{q}$ and W will be determined from the momentum and angle of the scattered electron. Each ring in Fig. 8 beginning at the center corresponds to $\Delta W = 1, 2, 3.., 10$ MeV. In the πN center of mass system the ring corresponds to constant pion momentum and is a function of the pion polar angle from $\theta_\pi^* = 0° - 180°$. The right hand part of the curves corresponds to $\phi_\pi = 0°$ and the left hand part to $\phi_\pi = 180°$. The black lines indicate the acceptance of BigBite in lab proton momentum and lab proton angle. The large vertical angular acceptance of BigBite ($\pm 18°$) allows full coverage of the pion polar CM angle $\theta_\pi^* = 0° - 180°$ for out of plane angles ϕ near 90° and 270° for $\Delta W = 0 - 20$ MeV. The horizontal angular acceptance of BigBite ($\pm 5°$) allows full coverage of the pion polar CM angle $\theta_\pi^* = 0° - 180°$ for in plane angles $\phi = 0°$ and 180° for $\Delta W = 0 - 5$ MeV. For other ϕ angles different portions of phase space are covered. In all cases the complete range of proton momenta are obtained.

Near threshold the data will be obtained in 1 MeV bins in ΔW from $\Delta W = 0 - 20$ MeV, and in Q^2 bins of 0.01 $(GeV/c)^2$ from $Q^2 = 0.04$ to 0.14 $(GeV/c)^2$. The angular distribution for each ΔW and Q^2 bin will be presented in 9 bins in θ and 18 bins in ϕ. Statistical uncertainties are expected to be on the level of 1-2% at angles where the cross section is maximum and 2.5% on the average. The beam energy and angles that will yield the largest cross sections near threshold for the above kinematics are shown in Table 2.

The required amount of beam time needed to obtain the desired statistics is based on the cross section calculations of MAID and SAID for the kinematics in Table 2. A luminosity

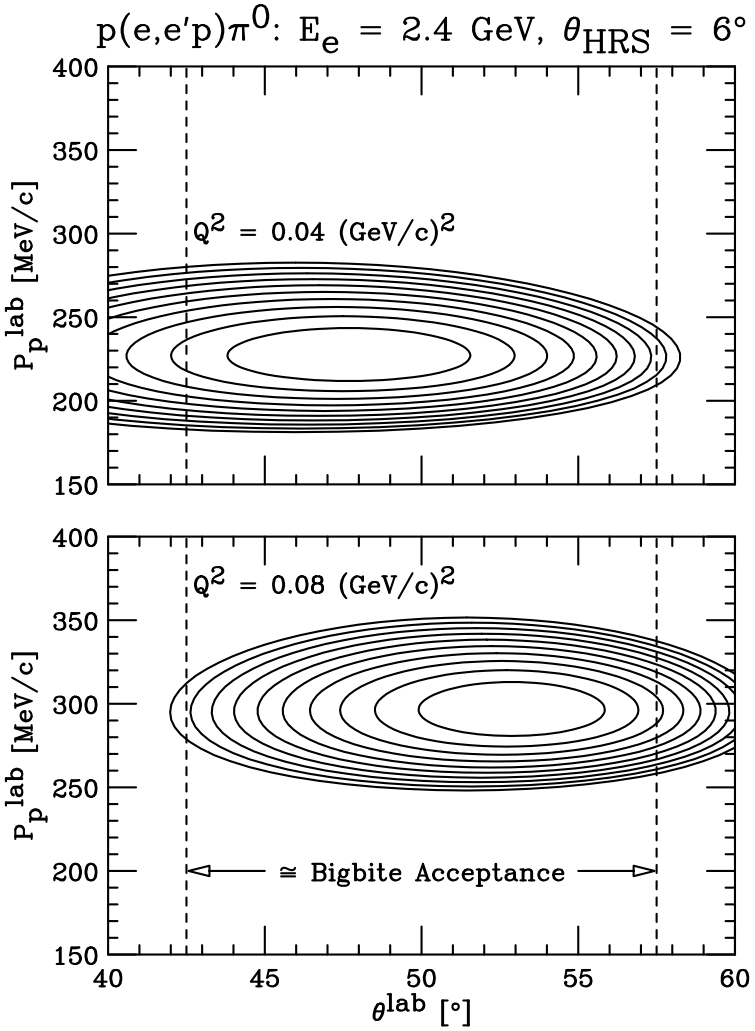

Fig. 8. The momentum of the emitted proton is plotted vs. the proton scattering angle in the lab for different values of ΔW for Q^2 = 0.04 and 0.08 $[GeV/c]^2$. The kinematic region which can be completely measured with a single setting of BigBite with a 10 cm extended target is indicated by the vertical black lines.

Table 2
Proposed kinematic settings showing the ranges in P_p, θ_e and θ_p for a fixed invariant mass W of 1074 MeV. Neither the BigBite spectrometer nor the HRS has to be moved to accommodate these kinematic ranges. The calculations were done for the standard Jefferson Lab beam energies.

Setting Number	E [MeV]	θ_e [degrees]	Q^2 $[MeV/c]^2$	W [MeV]	P_p [MeV/c]	θ_p [degrees]
1	2400	5.1 - 7.0	0.04 - 0.08	1074	215 - 275	45 - 54
2	3200	5.2 - 6.9	0.07 - 0.14	1074	270 - 340	50 - 57

of 1×10^{37} Hz/cm^2 is assumed and corresponds to a beam current of 5 uA and a target thickness of 0.7 gm/cm^2. Expected differential cross sections in the π-N center of mass system based on calculations from MAID are shown in Fig. 9 for various energies above threshold. The transverse plus longitudinal (T+L) and transverse-longitudinal interference

(TL) are extracted by a least squares fit to the simulated data with statistical errors of 1.7% and 3.6% respectively. These statistical errors would be typical for an assumed 100 hours of data taking. Although the cross section increases as energy increases above threshold, the acceptance of BigBite decreases and therefore the statistical errors increase significantly by the time you get to 20 MeV above threshold. The spectrometer central angles and the beamtimes are shown in Table 3.

Table 3
The beamtime table assumes a luminosity of $1 \times 10^{37}\ Hz/cm^2$. These settings will cover a Q^2 range of 0.04 - 0.14 $[GeV/c]^2$ in steps of 0.01(GeV/c)^2 and most of phase space for $\Delta W = 0 - 20$ MeV, and some portion of phase space for ΔW up to 200 MeV. The HRS and BigBite spectreometer will remain in a single configuration throughout the measurements. The estimated beam time assumes that we will obtain on average 2.5% statistics in each of 81 angular bins, 10 bins in Q^2, and several bins of ΔW (1 MeV wide) near threshold .

Setting Number	Beam Energy [MeV]	HRS Momentum [MeV]	HRS Angle [degrees]	BigBite Momentum [MeV]	BigBite Angle [degrees]	Beam Time [hours]
1	2400	2222	6.0	245	51.0	100
2	3200	2996	6.0	305	51.0	100

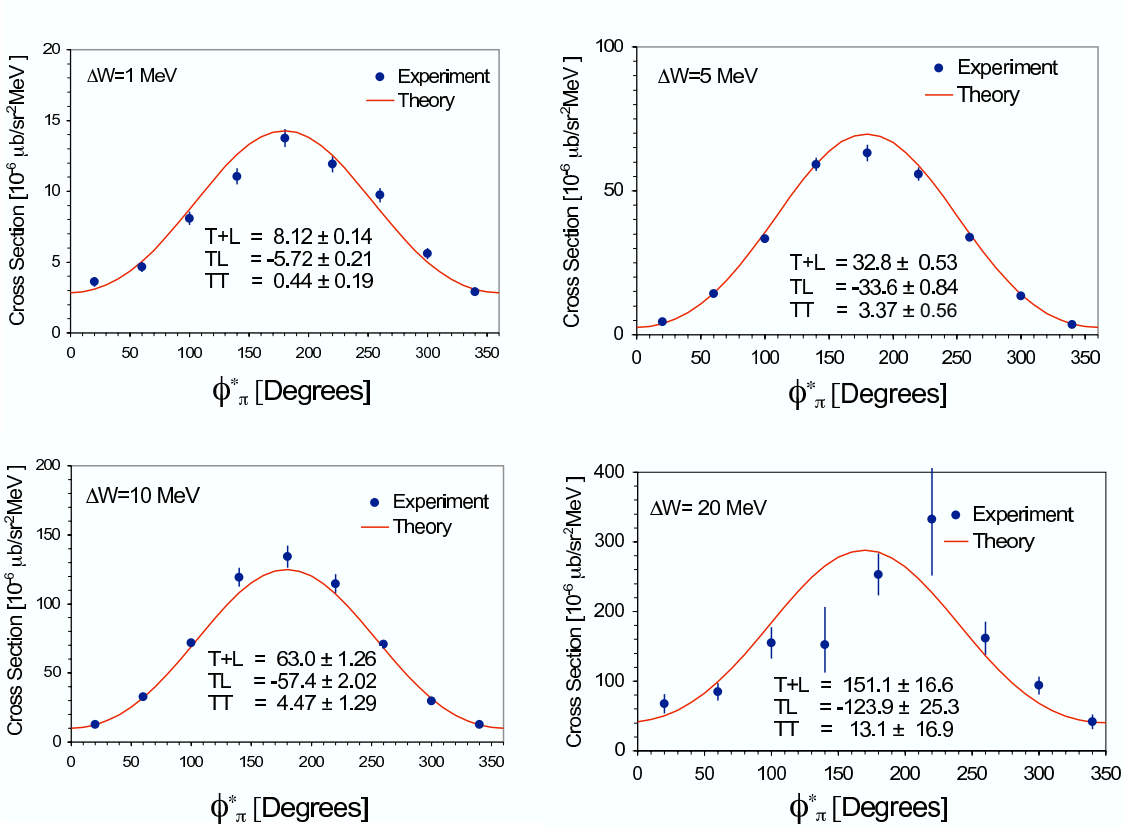

Fig. 9. Shown are a subset the expected differential cross sections and statistics for various energies above threshold obtained for the 2400 MeV beam energy setting, Q^2 = 0.04 - 0.05 $[GeV/c]^2$, and $\theta^* = 90°$. The differential cross sections are based on calculations from MAID.

To keep uncertainties in the reconstructed proton emission angles as small as possible, the amount of total material (target, windows, air, and detectors) traversed by the protons should be kept to a minimum. In the proposed setup, as shown in Fig. 12, the low energy protons travel out of the liquid hydrogen target through a thin Havar window separating the target from vacuum and through another thin Havar window (25 μm) separating the target from helium at atmospheric pressure before exiting through a 6 μm mylar foil into the drift chambers.

Table 4 shows Monte Carlo Geant simulation comparing this setup to one where BigBite is vacuum coupled to the target. These simulations were carried out for the lowest momentum protons 0.20 - 0.24 GeV/c of interest using the nominal magnetic field of 9 kG and tracks were reconstructed using front and back drift chambers. Results are also shown for the expected error in invariant mass and Q^2, which only depend on the electron variables. There is some improvement in σ_ϕ using vacuum over helium, but it is not significant. From Fig. 9, it can be seen that binning the data in roughly 20 degrees in θ^* and ϕ^* is sufficient to extract the cross sections of interest with statistical errors of the order of a few per cent. Also using using helium avoids having a large (30 cm x 125 cm) thin exit window separating vacuum from atmosphere just before the drift chambers. This would have the risk of imploding possibly destroying the costly drift chambers.

In order to identify a detected proton in BigBite with the production of a neutral pion, it is necessary to precisely determine the missing mass in the (e,e'p) reaction. The smaller the uncertainty on the measured missing mass the better the signal to noise and subsequent reduction of background. Figure 10 shows the distribution of the reconstructed events for the invariant mass W, the missing mass, and the angles in the center of mass expected in the experiment. The results indicate that the proposed setup meets the needs of the proposed experiment.

Table 4
Monte-Carlo Geant calculation for missing mass, invariant mass, and angular resolutions in c.m. of $\pi^\circ N$-system and Q^2 for $\Delta W = 1 - 2 MeV$ above threshold

Transport Medium	Window Thickness	$\sigma_{miss.mass}$ MeV	$\sigma_{\Delta W}$ MeV	$\sigma_{\Theta_{c.m.}}$ Degrees	σ_ϕ Degrees	σ_{Q^2} $(GeV/c)^2$
He Bag	25μm Havar	1.1	0.6	11°	12.5°	0.60×10^{-3}
Vacuum Chamber	150μm Kapton	1.0	0.6	10°	11°	0.56×10^{-3}

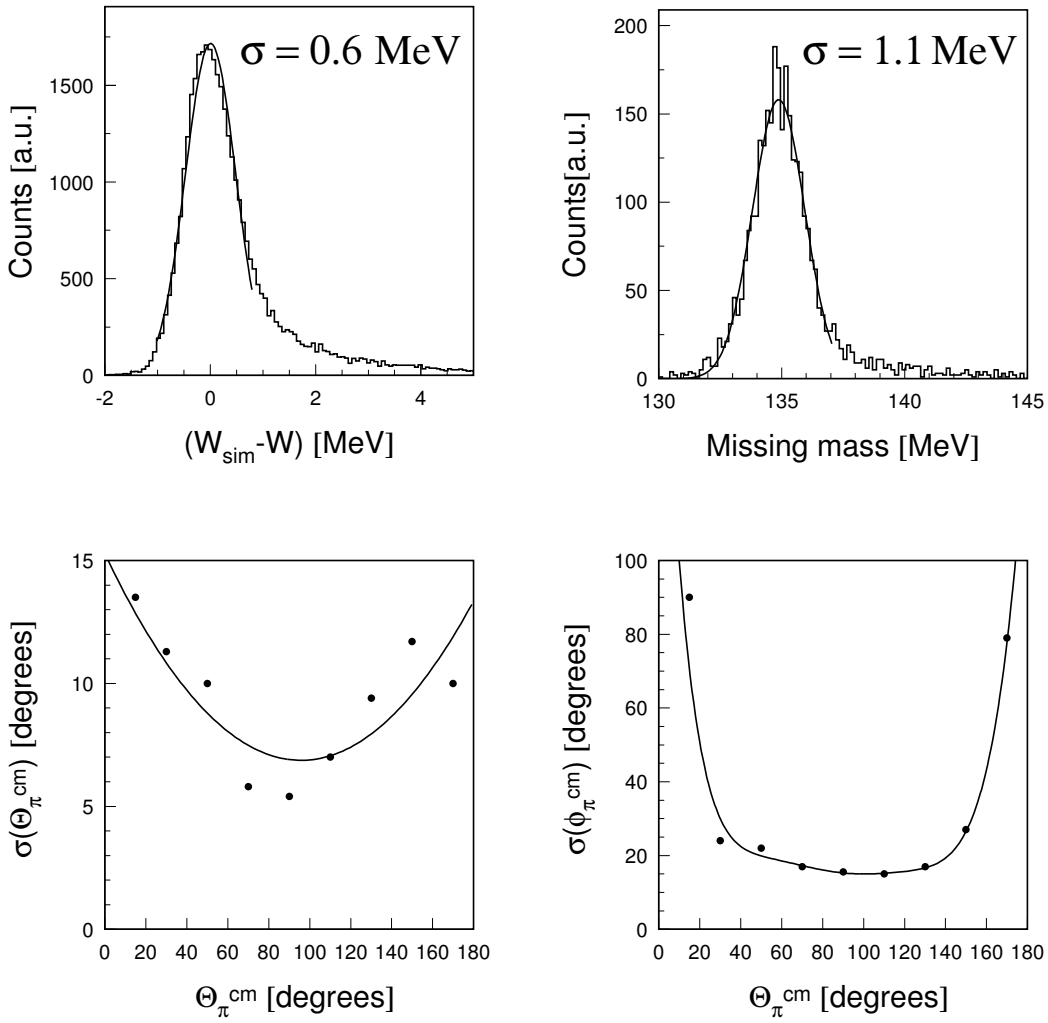

Fig. 10. Shown above is the expected missing mass resolution, the invariant mass W resolution, and the angular resolution of the reconstructed center of mass angles θ and ϕ. These results were generated using a GEANT Monte Carlo of the BigBite/HRS system including target and window thicknesses and two six-plane multi-wire drift counters.

At a luminosity of $10^{37} Hz/cm^2$, the total singles rate in BigBite has been calculated using a Monte Carlo cascade simulation program which also has been checked against parasitic experiments conducted in Hall A. Results from the calculation of singles rates for protons, π^+, π^-, gammas, and neutrons are shown in Fig. 11. From these measurements and calculations, we estimate that for an electron beam energy of 2.4 GeV the total proton singles rate in the BigBite solid angle will be approximately 1.5 MHz at a luminosity of $10^{37} Hz/cm^2$. Most of these events are low energy protons, around 200 MeV/c. This rate in first approximation is distributed uniformly over the acceptance and consequently over a plane of 170 sense wires, thus corresponding to about 9 kHz per wire. Since the drift velocity is the order of 100-300 ns, our count rates are well below the rate limitation of the chamber.

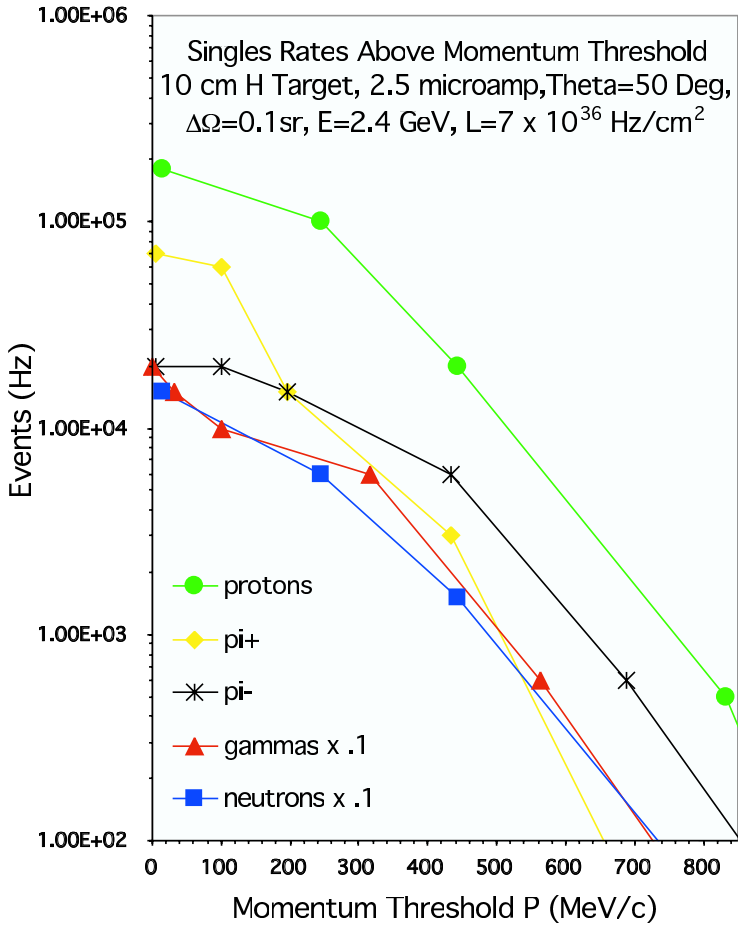

Fig. 11. Single rates above momentum threshold

In order to calibrate the large acceptance BigBite spectrometer, the electromagnetic calorimeter, which was built for experiment E99-114 [15], will be used. The calorimeter will be used to measure the energy and angle of elastically scattered electrons; the BigBite spectrometer will detect the recoiling proton. With the calorimeter, the energy and position of the detected electron can be determined with resolutions of better than $\sigma_{\delta E/E} = 0.01 + 0.06/\sqrt{E(GeV)}$ and 4.3 mm, respectively.

For calibrating BigBite with 800 MeV (1600 MeV) beam, the calorimeter will be positioned at 47° (33°) to detect elastic electrons in coincidence with recoil protons at 51° in BigBite as shown in Fig. 6. This will allow the BigBite spectrometer to be calibrated in situ, avoiding systematic errors related to moving it. The large out-of-plane acceptance of the BigBite spectrometer is well matched to the calorimeter's out-of-plane acceptance. Survey of the calorimeter with an accuracy of 1 mm will allow an absolute angular calibration of the BigBite spectrometer to accuracy of 0.2 mr.

The Hall-A ^{12}C multi-foil target will be used to calibrate the reconstruction of the target position of the BigBite spectrometer. Both the ^{12}C foils and 10 cm liquid targets will be used during the elastic scattering calibration measurements. Due to the large momentum acceptance of the BigBite spectrometer, we will make use of the elastic radiative tail to calibrate the entire momentum acceptance with a minimum number of different beam energies. This calibration will provide the momentum calibration to better than 0.5% and a recoil angle calibration precision of better than 1 mr. The calibrations will be performed at first with the BigBite magnetic field set to zero, in order to check the wire chamber resolutions. Then, the magnetic field will be turned to its nominal value of 0.92 T for the momentum calibration. These techniques are similar to those that were developed originally at NIKHEF to commission the BigBite spectrometer [10,11].

4.6 Luminosity Measurement

The target thickness-beam current product will be determined with an accuracy of about 1-2 % by measuring elastic scattering. This accuracy is sufficient for the proposed experiment. The relative luminosity during the pion production measurements will be monitored in the left right HRS to better than 1%. This technique of using elastic scattering followed by continuous luminosity monitoring has been used in Hall A during the E89-044 and E97-111 experiments.

5 Status of New Equipment

Along with the standard Hall A equipment, this experiment will require the large acceptance BigBite spectrometer, a scattering chamber with a large vertical opening to match the acceptance of the BigBite spectrometer, and a liquid hydrogen target cell with a thin cell wall. A schematic of this equipment is shown in Fig. 12. In this section, an overview of the status of this new equipment is presented.

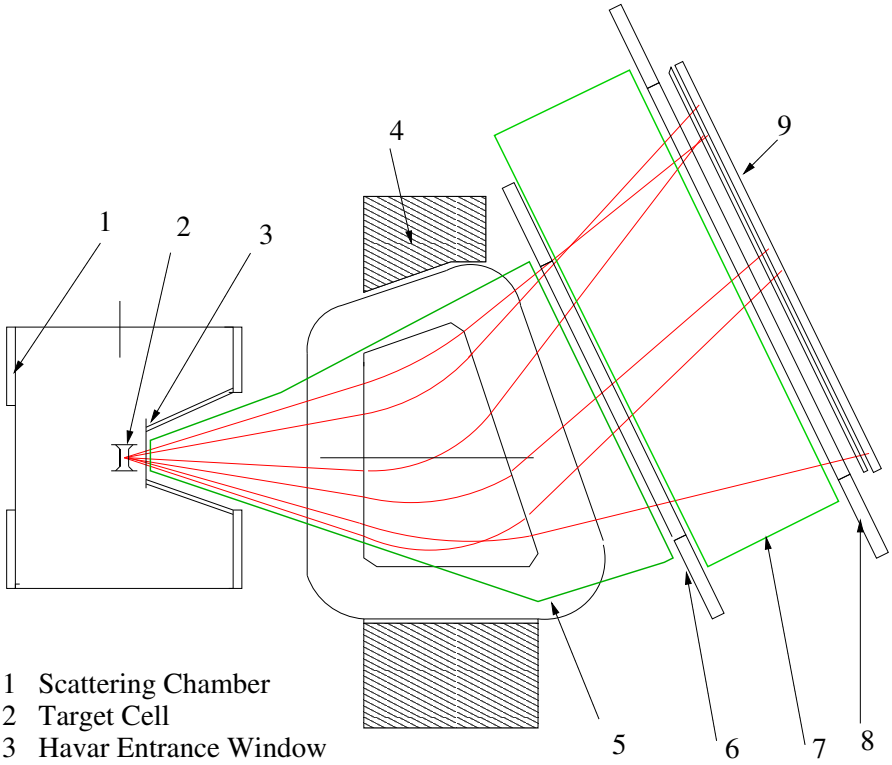

1 Scattering Chamber
2 Target Cell
3 Havar Entrance Window
4 BigBite Magnet
5 Helium Bag
6 Front Drift Chamber
7 Helium Bag
8 Back Drift Chamber
9 Trigger Scintillator Δ E–E Planes

Fig. 12. A layout of the new experimental equipment for the proposed experiment.

5.1 BigBite Spectrometer

Low energy protons from the reaction $^1H(e,e'p)\pi^0$ will be detected in the non-focusing BigBite spectrometer. The spectrometer consists of a large dipole magnet, multi-plane multi-wire drift chambers, and ΔE — E scintillator trigger planes. The BigBite spectrometer will have a nominal momentum acceptance of 0.2 GeV/c - 0.9 GeV/c and a nominal solid angle acceptance of 96 msr. Table 5 shows the properties of the BigBite spectrometer compared to one of the Hall A HRS spectrometers.

Table 5
Comparison of the characteristics of the BigBite spectrometer to one of the Hall A HRS.

Device	Momentum Acceptance [%]	H Angular Acceptance [mr]	V Angular Acceptance [mr]	Solid Angle [msr]	Δp/p	$\delta\theta_H$ [mr]	$\delta\theta_V$ [mr]	σ_{vertex} [cm]
BigBite	80	$\pm$80	$\pm$300	96	5×10^{-3}	3.2	3.2	0.32
HRS	10	$\pm$20	$\pm$60	6.2	1×10^{-4}	1.0	2.0	0.1

5.1.1 Magnet and Platform

The BigBite spectrometer dipole magnet was originally used at NIKHEF in the internal target hall [10,11] and is currently located in Hall A. In order to position the magnet and detector packages, a customized stand and detector carriage have been constructed and are currently being pre-assembled in Hall A. The platform will allow the BigBite spectrometer to be rotated to arbitrary angles and allow the magnet to be positioned as close as 1 m from a target.

5.1.2 Drift Chambers

In order to take full advantage of the high luminosities at Jefferson Lab, BigBite will be instrumented with multi-wire drift chambers. The chambers will consists of sets of u,v and x planes together with fast readout electronics. The x plane will give us position resolution of the order of 0.2 mm in the dispersive plane. The u and v planes are oriented at $\pm$ 30 degrees to the x plane and will give position information in both the transverse plane and the dispersive plane. The second set of planes u', v' and x' provide information to eliminate right/left ambiguities and to add redundancy, permitting good track identification even if some wires do not fire.

The chambers are currently under construction at the University of Virginia. Figure 13 shows a photograph of one of the planes during construction. Jefferson Lab has purchased CAEN V767 multihit TDC units for reading out the wire chambers. These units have been incorporated into a VME data acquisition system and will be used both to test the chambers and in the final data acquisition system. Once all the chambers have been built and tested at the University of Virginia, they will be transported to Jefferson Lab to be incorporated into a detector package with the trigger scintillators.

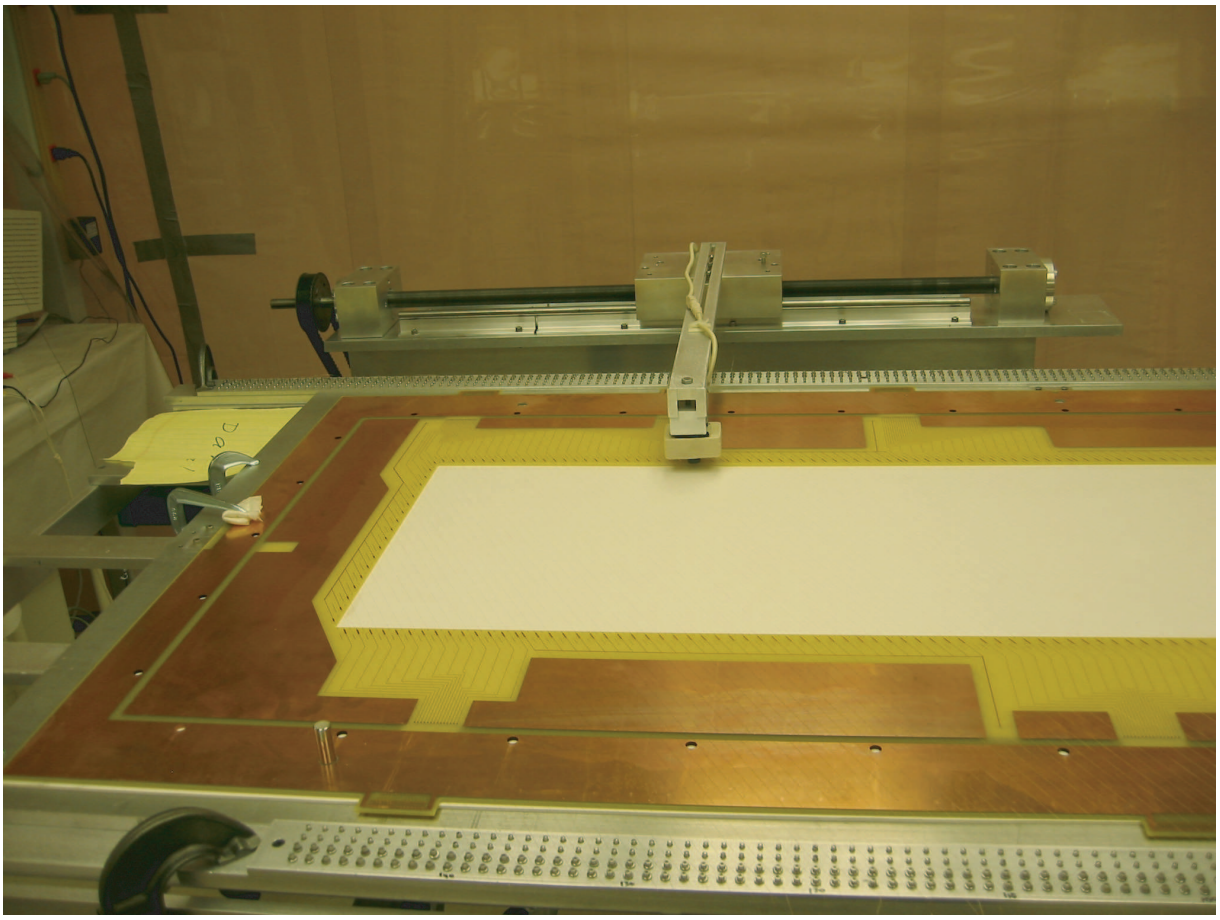

Fig. 13. Shown is a typical plane of one of the BigBite drift chambers. In this plane, the signal and field wires are inclined at 30 degrees. A small motorized camera connected to a computer is used to measure wire spacing.

5.1.3 Δ E and E Scintillator Trigger planes

For the π^0 experiment, rates in the trigger plane will be of the order of 1 MHz, necessitating a highly segmented trigger scintillation detection system. This system is comprised of 3 mm thick and 30 mm thick scintillation planes. Each plane is segmented into 24 elements with each element read out via light guides by two fast 50 mm photomultiplier tubes. The 30 mm thick layer will provide timing resolution of better than 0.5 ns while the ΔE/E information from the two planes together will provide particle identification information. Fig. 14 shows a CAD drawing of the scintillators along with a photograph of the system during its construction. the trigger plane has been constructed and is currently undergoing testing.

Fig. 14. Scintillation counters used for the BigBite trigger ΔE/E detectors

An exploded view of the new scattering chamber system and associated flanges is shown in Fig. 15. The principal component of the scattering chamber is the aluminum middle ring which has large openings on each side to match the large vertical acceptance of the BigBite spectrometer. For this experiment, the curved flange on the left side in the figure will contain a thin foil for electrons and the flange on the right side will contain a port for coupling to a Helium bag. The steel base ring and the septum extension have already been constructed and used in Hall A.

This new chamber was designed by the Jefferson Lab design group and is currently under construction at a local machine shop. The chamber will be hydrotested and leak checked before delivery. All parts are expected to be delivered to Jefferson Lab by early 2004.

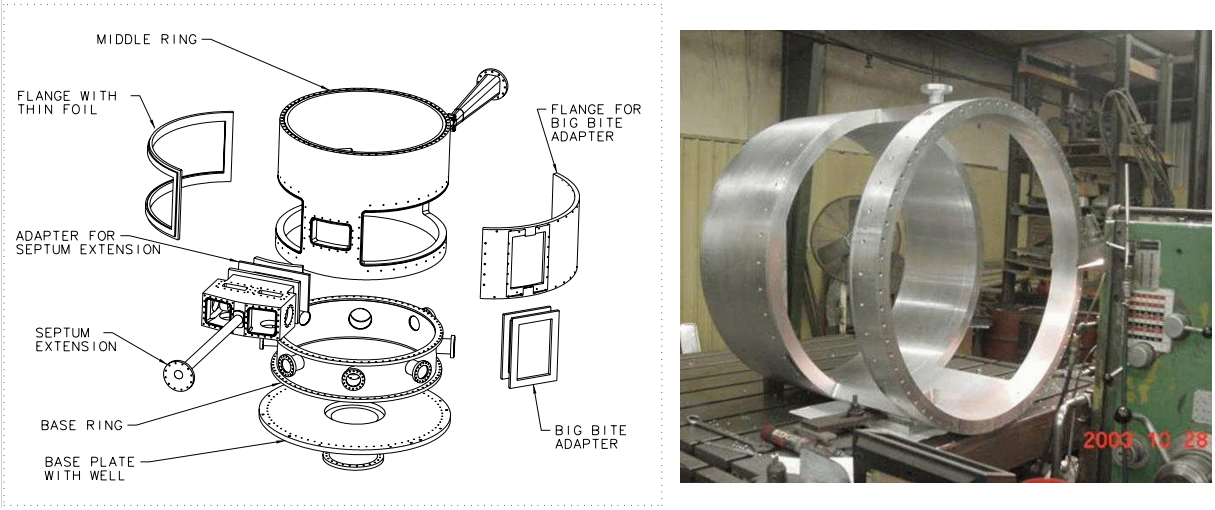

Fig. 15. Shown is an exploded view of the new scattering chamber being built for use with the BigBite spectrometer along with a photograph taken during construction. The side openings of this chamber are twice as high as the present Hall A scattering chamber in order to match the large out-of-plane acceptance of the BigBite spectrometer.

For the threshold pion experiment, the standard Hall A liquid hydrogen cylindrical target cell will need to be replaced by a cell with windows made out of 10 μ Havar foil. This new Havar cell, which will be 10 cm long and 2 cm wide, will minimize the amount of material the low energy exiting protons (typically 20 - 30 MeV) will pass through to minimize straggling and multiple scattering. The cell will also have Havar beam entrance and exit foils, so will produce less background than the normal Hall A cell. A prototype cell made with aluminum has been constructed by Dave Meekins of the Jefferson Lab target group and is shown in Fig. 16 .

The prototype cell proved to be leak tight well over the necessary bursting pressure of 100 psi and the Havar cell is expected to be even stronger. The final cell will be composed of a Havar foil with a copper cell block and stainless transitions to the cryotarget plumbing. With the successful test of the prototype cell, we do not expect any problems with the construction of the final cell.

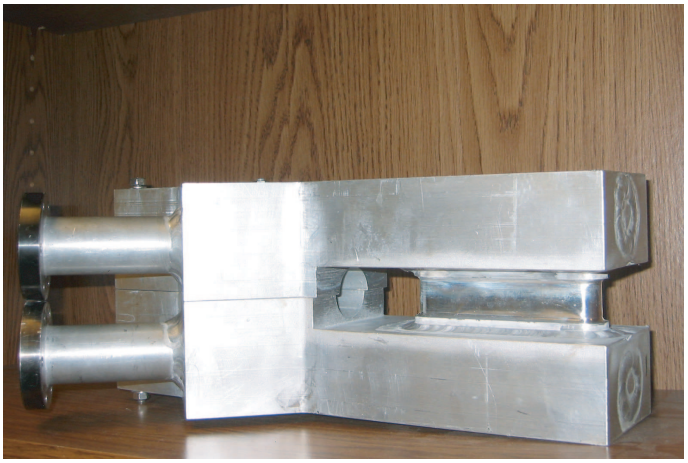

Fig. 16. Shown is the prototype liquid hydrogen target. The 10 cm cell is located on the right side between the aluminum jaws.

6 Funding and Manpower

In January of 2001, the Jefferson Lab Program Advisory Committee (PAC) approved the first two BigBite experiments. One was a proposal to measurement short range correlations (SRC) via the triple coincidence ^{12}C(e,e'p+N) reaction and the other was the threshold pion production experiment described herein. After the PAC results were known, the members of the two experiments joined forces to create the BigBite working group. Since the SRC experiment could be completed without wirechambers, the working group decided to focus its energy on completing the equipment needed for the SRC experiment while pursuing funding for new wire chambers.

In June 2002, the sum of $441,000 from the NSF Major Research Instrumentation (MRI) program was awarded to the University of Virginia (Award Number PHY-0216351) for the development and instrumentation of the large acceptance BigBite spectrometer and associated experimental apparatus. A major portion of these funds is being used to construct the multi-plane multi-wire drift chambers and the new scattering chamber. In addition to MRI funding, the University of Glasgow has committed over $250,000 for the trigger plane and associated electronics. Tel Aviv University has also contributed over $50,000 to build an auxiliary scintillator plane which will be used in lieu of wirechambers during the SRC experiment. The Massachusetts Institute of Technology has supported these project with graduate students and research associates. Jefferson Laboratory has contributed manpower, funds, electronics (such as the multi-hit TDC's for the BigBite wirechambers) and has provided much of the design work for the project.

7 Beamtime

We propose an experiment that is a precision test of ChPT. This experiment requires a careful calibration of the BigBite spectrometer in order to precisely measure the pion production cross sections near threshold. Once calibrated, two different beam energies will be used to measure the cross sections and response functions from a Q^2 of 0.04 thru 0.14 $[GeV/c]^2$ without moving either spectrometer. As shown in Table 6, a total of 16 days is requested to complete the experimental program. The 100 hrs needed for the two sets of kinematics has been increased by 20% to account for the nominal 20% computer and electronic deadtime.

Table 6
Time requested for experiment and calibration of the BigBite spectrometer. The calibration measurements will be done with 800 MeV and 1600 MeV beam and physics measurements we be done with 2400 MeV and 3200 MeV.

Cross Section Measurements	240 hrs
Energy Changes (1)	16 hrs
Energy Measurements	16 hrs
Subtotal	272 hrs
Calibration Measurements	80 hrs
Energy Changes (1)	16 hrs
Energy Measurements	16 hrs
Subtotal	112 hrs
Total	384 hrs (16days)

References

[1] H.W. Hammer U-G. Meissner and A. Wirzba, editors, *Mini-Proceedings of the Fourth International Workshop on Chiral Dynamics: Theory and Experiment*, 2003.

[2] M.Fuchs *et al.*, Phys. Lett. **B368** (1996) 20.

[3] J.C. Bergstrom *et al.*, Phys Rev. **C53** (1996) R1052.

[4] M.O.Distler *et al.*, Phys. Rev. Lett. **80** (1998) 2294.

[5] H. Merkel, Pion threshold electro- and photo- production, Talk for the Chiral Dynamics 2000 Workshop.

[6] H. Merkel *et al.*, Phys. Rev. Lett. **88** (2002) 12301.

[7] W.J. Briscoe R. A. Arndt, I. I. Strakovsky and R. L. Workman, Phys. Rev. **C66** (2002) 055213.

[8] I.I. Strakovsky R. A. Arndt, W.J. Briscoe and R.L. Workman, in *Proceedings of the Workshop on the Physics of Excited Nucleons (NSTAR2002)*, edited by S.A. Dytman and E.S. Swanson, World Scientific, 2003.

[9] D. Drechsel, O. Hanstein, S. S. Kamalov and L. Tiator, Nucl. Phys. **A645** (1999) 145.

[10] D.J.J. de Lange *et al.*, Nucl. Instr. and Meth. **A 406** (1998) 182.

[11] D.J.J. de Lange *et al.*, Nucl. Instr. and Meth. **A 412** (1998) 254.

[12] K. Kumar *et al.*, Constraning the nucleon strangeness radius in parity violating electron scattering, TJNAF Proposal E99-115.

[13] D. Amrstong *et al.*, Parity violation from ^4He at low q^2: A clean measurement of ρ_s, TJNAF Proposal E00-114.

[14] R. Michaels, A clean measurement of the neutron skin of ^{208}Pb through parity violating electron scattering, TJNAF Proposal E00-003.

[15] C. Hyde-Wright *et al.*, Exclusive compton scattering on the proton, TJNAF Proposal E99-114.

[16] U.-G. Meissner, Chiral QCD: Baryon dynamics, in *Encyclopedia of Analytic QCD*, edited by World Scientific M. Schifman, 2000.

[17] V. Bernard, N. Kaiser and Ulf-G. Meißner, Nucl. Phys. **A607** (1996) 379.

[18] V. Bernard, N. Kaiser and Ulf-G. Meißner, Nucl. Phys. **A633** (1998) 695.

[19] T.P. Welch *et al.*, Phys. Rev. Lett. **69** (1992) 2761.

[20] V. Bernard *et al.*, Z. Phys **C70** (1996) 483.

[21] V. Bernard, N. Kaiser and Ulf-G. Meißner, Phys. Rev. Lett. **74** (1995) 3752.

[22] R. A. Arndt, I. I. Strakovsky and R. L. Workman, Phys. Rev. **C53** (1996) 430.

[23] R. A. Arndt, R. L. Workman, Zh. Li and L. D. Roper, Phys. Rev. **C42** (1990) 1853.

[24] H.B. van den Brink *et al.*, Nucl. Phys. **A612** (1997) 391.

[25] D. Drechsel and L. Tiator, J. Phys. G: Nucl. Part. Phys. **18** (1992) 449.